様　式　Ｃ－１９、Ｆ－１９－１、Ｚ－１９　（共通）

科学研究費助成事業　　研究成果報告書

令和　３ 年 １０ 月 ２０ 日現在

機関番号：８２１０８
研究種目：若手研究(B)
研究期間：2017～2018
課題番号：１７Ｋ１４６５２

研究課題名（和文）Fabrication of Weyl semimetals based spintronic heterostructures for future energy-efficient IT devices

研究課題名（英文）Fabrication of Weyl semimetals based spintronic heterostructures for future energy-efficient IT devices

研究代表者

温　振超（Wen, Zhenchao）

国立研究開発法人物質・材料研究機構・磁性・スピントロニクス材料研究拠点・主任研究員

研究者番号：４０７８４７７３

交付決定額（研究期間全体）：（直接経費）　　3,300,000円

研究成果の概要（和文）：The Weyl semimetal films of WTe2 and MoTe2 were fabricated by sputtering for the first time. A sizeable spin Hall effect was achieved in the Weyl semimetals. Furthermore, Co2MnGa Weyl semimetal thin films were fabricated and the degree of order dependence of anomalous Hall effect was discovered.

研究成果の学術的意義や社会的意義
The experimental demonstration of the spin-orbit effects in Weyl semimetals in this research can contribute the progress of the developments of topological spintronic devices, which could provide an essential way of achieving energy-efficient IT devices for realizing the super-smart society.

研究成果の概要（英文）：In this research, the Weyl semimetal films of WTe2 and MoTe2 were fabricated by sputtering for the first time. By combining with CoFeB/AlOx, spin Hall magnetoresistance was investigated. A sizeable spin Hall effect was achieved in the sputtered WTe2 Weyl semimetal based spintronic structures. Furthermore, Co2MnGa Weyl semimetal thin films were fabricated by sputtering method and the spin-orbit effects in the films were studied. A large anomalous Hall angle of ~14% was achieved. It is also observed that the anomalous Hall effect strongly depends on the degree of order of the Co2MnGa Weyl semimetals. The samples containing L21-ordered phase show enhanced anomalous Hall effect compared to B2-ordered samples. The reason could be the different electronic structures between the two ordered phases. The experimental demonstration of the spin orbit effects in sputtered Weyl semimetals could contribute the progress of the development of topological spintronic devices.

研究分野：磁性・スピントロニクス材料

キーワード：Weyl semimetals　Spintronic structures　Spin-orbit effects

１．研究開始当初の背景

Energy-efficient and environment-friendly information technology (IT) devices are indispensable for establishing a super-smart and sustainable society. However, the properties of conventional materials are limited to further improve the performance of IT devices and cannot satisfy the energy-efficient memory and computing. Developing high-performance spintronic materials/heterostructures is an essential way of achieving future energy-efficient IT devices for realizing super-smart systems with various functionalities.

２．研究の目的

The purpose of this research is to design and fabricate Weyl semimetals (WSs) based spintronic heterostructures for achieving high-performance and energy-efficient spintronic devices. The Weyl semimetal is a topologically nontrivial phase of matter that was discovered recently. Because of a large Berry curvature in their band structures, the WSs have been theoretically predicted to have large spin-orbit effects. Experimental demonstration of the WSs-based spintronic devices in this research will be of particular importance for realizing super-smart systems, such as internet of things (IoT) and artificial intelligence (AI) networks.

３．研究の方法

According to the condition of our laboratory, we fabricate the WS films (WTe_2, $MoTe_2$, and Co_2MnGa) using magnetron sputtering system with in-situ annealing process. The magnetron sputtering technique is beneficial for massive production with low cost and easy controllability, which is compatible with current industrial processes. In our research, the WTe_2 ($MoTe_2$) and Co_2MnGa films are sputtered from a W(Mo)-Te target and a Co-Mn-Ga target respectively in an ultrahigh vacuum sputter system. The in-situ annealing temperature during the deposition ranges from room temperature to 600 °C. The surface morphology of the films is characterized by atomic force microscope (AFM). The uniformity and crystalline quality of the films is examined by reflection high energy electron diffraction (RHEED) and x-ray diffraction. Furthermore, the samples are patterned into Hall bars and the transport properties are measured using physical properties measurement system (PPMS).

４．研究成果

(1) A sizeable spin Hall effect in sputtered WTe2 Weyl semimetal based spintronic structures.

The films of WTe2 and MoTe2, were fabricated by sputtering. The structural properties were characterized by x-ray diffraction (XRD), as shown in Figure 1. In addition to the peaks from the substrates, there is no clear peak observed in the XRD patterns, which indicates the 30-nm-thick films have an amorphous-like structure. A ferromagnetic layer of CoFeB with AlOx capping layer was deposited on the WTe_2 with varying thickness from 2 to 8 nm. Furthermore, Hall bar structures were microfabricated for the measurement of spin Hall magnetoresistance (SMR). The illustration of SMR measurement and Hall bar image are shown in Figure 2(a) and 2(b). A SMR ratio of ~0.05% was observed in the sample of WTe_2(2 nm)/CoFeB(2.5 nm)/AlOx at room temperature, as shown in Figure 2(c), which is comparable to that in the Pt/YIG system. By fitting the thickness dependence of the SMR, the spin Hall angle of WTe_2 was estimated to be ~-0.04 with a spin diffusion length of 2.5 nm at room temperature. The experimental demonstration of the spin orbit effect in sputtered WSs could contribute the progress of the development of WS-based spintronic devices.

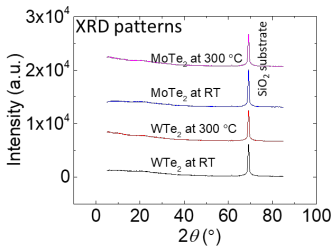

Figure 1, XRD patterns for the WTe2(30 nm) and $MoTe_2$(30 nm) deposited at room temperature and 300 °C, respectively.

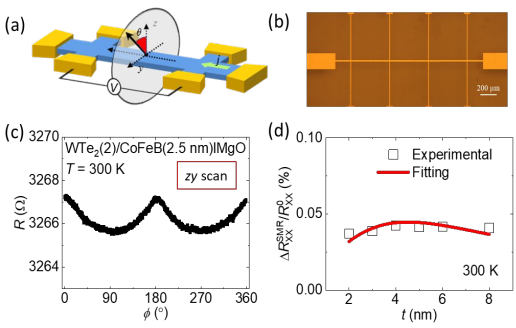

Figure 2, SMR in the WTe2/CoFeB/AlOx heterostructures. (a,b) illustration and image of Hall bar. (c) SMR raw data. (d) WTe_2 thickness dependence of SMR.

(2) Discovery of the degree of order dependence of AHE in Co_2MnGa Weyl semimetal thin

films.

The Co_2MnGa films with the thickness of 30 nm were deposited by the sputter system at different deposition temperatures of RT, 200 ºC, 400 ºC, 500 ºC and 600 ºC, respectively. The structures of the thin films were characterized by XRD with out-of-plane and in-plane scans. Figure 3(a) shows the out-of-plane XRD patterns for the series of samples. The (002) and (004) peaks were observed for all the samples deposited regardless of the deposition temperature, which indicates the films were grown along (001) orientation on the MgO(001) substrates. The intensity of the peaks increases with the increase of deposition temperature, which could be due to the increased degree of order at high deposition temperatures. Figures 3(b) shows the XRD patterns for the 111 peaks, which were detected by tilting the samples to $\chi = 54.7°$. For the thin films deposited at RT and 200 ºC, no (111) peaks were observed. With increasing the deposition temperature, the (111) peak appeared and was clearly observed at the temperatures of 500 ºC and 600 ºC. The intensity of the peak increased with the deposition temperature, indicating the increased degree of order at high deposition temperatures. The degree of order of the samples were plotted as a function of deposition temperature, as shown in Fig. 3(c). The Co_2MnGa films possess two kinds of ordering structures: $L2_1$ and $B2$ structures. The degree of order for $B2$ structure increases with increasing the deposition temperature from RT to 400 ºC, then is nearly saturated with a degree of $B2$-ordering of ~80% from 400 ºC to 600 ºC. The degree of order for $L2_1$ structure starts to increase at 400 ºC. The maximum degree of $L2_1$-ordering of 40% was achieved in the sample deposited at 600 ºC.

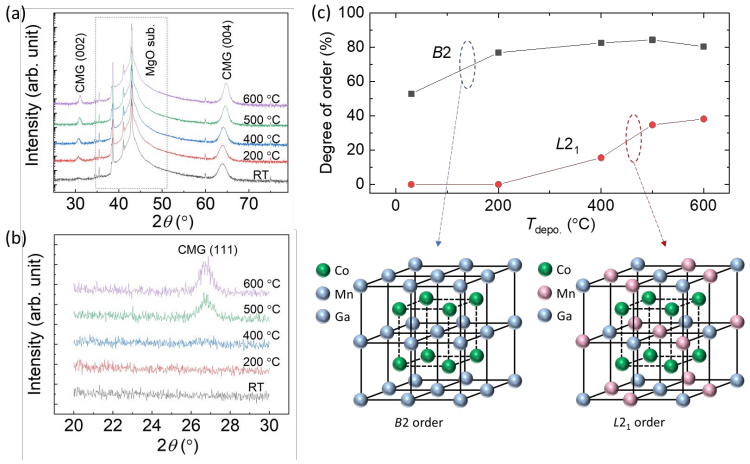

Figure 3, The degree of order of Co_2MnGa as a function of annealing temperature. (a) XRD out-of-plane scan. (b) XRD patterns for CMG111 peaks. (c) T_{depo} dependence of the ordering degree of CMG.

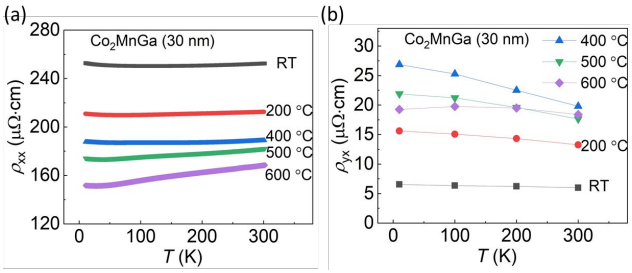

Figure 4, The temperature dependence of (a) longitudinal resistivity and (b) anomalous Hall resistivity for 30-nm-thick Co_2MnGa deposited at different temperatures.

Figure 4(b) shows the dependence of longitudinal resistivity on the measurement temperature. For the samples deposited RT, the longitudinal resistivity is nearly independent of measurement temperature. It is found that the difference of the longitudinal resistivities between 10 K and 300 K increases with increasing the deposition temperature. For the sample deposited at 600 °C, the longitudinal resistivity decreases with the decrease of measurement temperature. Figure 4 (c) shows the dependence of anomalous Hall resistivity on the measurement temperature. The transverse resistivity increases with decreasing the measurement temperature. Figure 5 indicates the dependence of anomalous Hall angle on the measurement temperature. Large anomalous Hall angles were achieved for the samples deposited at 400 ºC, 500 ºC, and 600 ºC. Considering the ordering structure, it is found that the samples containing $L2_1$ order show enhanced AHE compared to B2-ordered samples, which could be attributed to the electronic band structures. By further investigating the dependence of Hall conductivity on longitudinal conductivity, we found

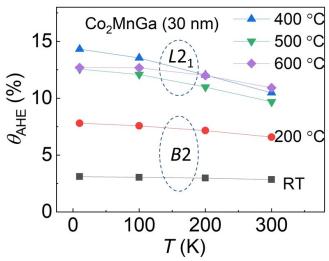

Figure 5, Anomalous Hall angle as a function of temperature with $L2_1$ and $B2$ ordered phases.

that the dominant contribution to AHE is the intrinsic contribution. This research can contribute to the design of WSs-based materials with large spin-orbit effects by structural order control.

５．主な発表論文等

〔雑誌論文〕（計 7 件）

① H. Sharma, **Z. C. Wen**, K. Takanashi, and M. Mizuguchi
Anomaly in anomalous Nernst effect at low temperature for C1b-type NiMnSb half-Heusler alloy thin film
Jpn. J. Appl. Phys. **58**, SBBI03 (2019). 10.7567/1347-4065/aafe68/meta (査読有り)

② T. Kubota, Y. Ina, **Z. C. Wen**, and K. Takanashi
Temperature dependence of CPP-GMR in the junctions with interface tailored Heusler alloy electrodes
J. Magn. Magn. Mater. **474**, 365 (2019). 10.1016/j.jmmm.2018.11.051 (査読有り)

③ **Z. C. Wen**, T. Kubota, and K. Takanashi
Optimization of half-Heusler PtMnSb alloy films for spintronic device applications
J. Phys. D: Appl. Phys. **51**, 435002 (2018). 10.1088/1361-6463/aadf4e/meta (査読有り)

④ **Z. C. Wen**, T. Kubota, and K. Takanashi
Epitaxial CuN films with highly tunable lattice constant for lattice-matched magnetic heterostructures with enhanced thermal stability
Adv. Electron. Mater. **3**, 1700367 (2018). 10.1002/aelm.201700367 (査読有り)

⑤ T. Kubota, Y. Ina, **Z. C. Wen**, and K. Takanashi
Interface tailoring effect for Heusler based CPP-GMR with an $L1_2$-type Ag_3Mg spacer
Materials **11**, 219 (2018). 10.3390/ma11020219 (査読有り)

⑥ **Z. C. Wen**, H. Sukegawa, T. Seki, T. Kubota, K. Takanashi, and S. Mitani
Voltage control of magnetic anisotropy in epitaxial Co_2FeAl/MgO heterostructures
Sci. Rep. **7**, 45026 (2017). 10.1038/srep45026 (査読有り)

⑦ T. Kubota, Y. Ina, **Z. C. Wen**, H. Narisawa, and K. Takanashi
Current perpendicular-to-plane giant magnetoresistance using an $L1_2$-Ag_3Mg spacer and $Co_2Fe_{0.4}Mn_{0.6}Si$ Heusler alloy electrodes: Spacer thickness and annealing temperature dependence
Phys. Rev. Mater. 1, 044402 (2017). 10.1103/PhysRevMaterials.1.044402 (査読有り)

〔学会発表〕（計 6 件）

① Q. Wang, **Z. C. Wen**, T. Seki, and K. Takanashi
Investigation of anomalous Hall effect in Co2(Fe, Mn)Si Heusler alloy films with tunable electronic structures
2019 **応用物理学会 春季学術講演会**

② T. Kubota, **Z. C. Wen**, and K. Takanashi
Anomalous Hall effects in five-elements Heusler alloy, Co2(Fe-Mn)(Al-Si) films
2019 Joint MMM-INTERMAG Conference, 2019

③ **Z. C. Wen**, T. Kubota, and K. Takanashi
CPP-GMR devices using C1b-type half Heusler alloys
第 42 **回日本磁気学会学術講演会**, 2018

③ **Z. C. Wen**, T. Kubota, and K. Takanashi
Optimization of half-Heusler PtMnSb alloy films for spintronic device applications

International Conference on Magnetism (ICM 2018), 2018

④ **Z. C. Wen**, Z. Qiu, T. Seki, D. Hou, T. Kubota, E. Saitoh, K. Takanashi
Inverse spin Hall effect in half-Heusler NiMnSb alloy films
5th International Conference of Asian Union of Magnetics Societies (IcAUMS 2018)

⑤ **Z. C. Wen**, T. Kubota, Y. Ina, and K. Takanashi
Dual-spacer nanojunctions exhibiting large current-perpendicular-to-plane giant magnetoresistance for ultrahigh density magnetic recording
62nd Annual Conference on Magnetism and Magnetic Materials, 2017

⑥ T. Kubota, Y. Ina, **Z. C. Wen**, and K. Takanashi
Layer Thickness Dependence of CPP-GMR in Co2Fe0.4Mn0.6Si | L12-type Ag-Mg | Co2Fe0.4Mn0.6Si Devices
Intermag 2017